Extracellular organic carbon dynamics during a bottom-ice algal bloom (Antarctica)

Sarah C. Ugalde[1,2,*], Andrew Martin[3], Klaus M. Meiners[1,4], Andrew McMinn[2], Ken G. Ryan[3]

[1]Antarctic Climate and Ecosystems Cooperative Research Centre, Private Bag 80, Hobart, Tasmania 7001, Australia
[2]Institute for Marine and Antarctic Studies, Private Bag 129, Hobart, Tasmania 7001, Australia
[3]School of Biological Sciences, Victoria University of Wellington, PO Box 600, Wellington 6140, New Zealand
[4]Australian Antarctic Division, Department of the Environment, 203 Channel Highway, Kingston, Tasmania 7050, Australia

ABSTRACT: Antarctic fast ice provides a habitat for diverse microbial communities, the biomass of which is mostly dominated by diatoms capable of growing to high standing stocks, particularly at the ice–water interface. While it is known that ice algae exude organic carbon in ecologically significant quantities, the mechanisms behind its distribution and composition are not well understood. This study investigated extracellular organic carbon dynamics, microbial characteristics, and ice algal photophysiology during a bottom-ice algal bloom at McMurdo Sound, Antarctica. Over a 2 wk period (November to December 2011), ice within 15 cm from the ice–water interface was collected and sliced into 9 discrete sections. Over the observational period, the total concentrations of extracellular organic carbon components (dissolved organic carbon [DOC] and total carbohydrates [TCHO] — the sum of monosaccharides [CHO_{Mono}] and polysaccharides [CHO_{Poly}]) increased, and were positively correlated with algal biomass. However, when normalised to chlorophyll *a*, the proportion of extracellular organic carbon components substantially decreased from initial measurements. Concentrations of DOC generally consisted of <20% TCHO, typically dominated by CHO_{Mono}, which decreased from initial measurements. This change was coincident with improved algal photophysiology (maximum quantum yield) and an increase in sea-ice brine volume fraction, indicating an increased capacity for fluid transport between the brine channel matrix and the underlying sea water. Our study supports the suggestion that microbial exudation of organic carbon within the sea-ice habitat is associated with vertical and temporal changes in brine physicochemistry.

KEY WORDS: Antarctica · Carbohydrates · Dissolved organic carbon · Microalgae · Nutrient limitation · Photophysiology · Sea ice

INTRODUCTION

Antarctic sea ice, permeated by a system of brine-filled pockets and channels, provides an extensive habitat for diverse microbial assemblages that play a significant role in the ecology and biogeochemistry of the Southern Ocean (Palmisano & Garrison 1993, Thomas & Dieckmann 2010, Vancoppenolle et al. 2013). The most conspicuous fast-ice-bound organ-

isms are microalgae (hereafter referred to as 'algae'; Arrigo et al. 2010) that form communities that are usually densest near the ice–water interface. These are referred to as bottom-ice communities (Thomas & Dieckmann 2010), and are able to achieve high biomass due to their proximity to inorganic nutrients in the underlying water column (McMinn et al. 1999, Kattner et al. 2004). Consequently, chlorophyll *a* (chl *a*) concentrations in the bottom ice can exceed

*Corresponding author: sarah.ugalde@utas.edu.au

300 mg m^{-2} (Palmisano & Sullivan 1983, Trenerry et al. 2002, Arrigo et al. 2010).

High concentrations of chl a in sea ice are often correlated with copious extracellular organic carbon, which is exuded by sea-ice algae and other microbes (e.g. Krembs et al. 2002, Meiners et al. 2004, Underwood et al. 2010, 2013). The ecological functions of the high extracellular organic carbon in sea ice remain unclear. It might aid in cell motility and attachment (Hoagland et al. 1993, Underwood & Paterson 2003), or provide a protective coating, which may be a mechanism to cope with variable physicochemical conditions including low temperature, salinity, pH, or nutrient concentrations (Krembs et al. 2002, Krembs & Deming 2008, Krembs et al. 2011, Ugalde et al. 2013). Alternatively, the high degree of metabolic activity in ice-associated bacteria (Martin et al. 2008, 2009, Meiners et al. 2008) and tight seasonal coupling between the relative abundance of bacteria and algae is suggestive of an active microbial loop, similar to that of temperate oceanic systems (Sullivan & Palmisano 1984, Azam et al. 1991, Smith et al. 1995, Christaki et al. 1998). This relationship may develop when bacteria assimilate extracellular organic carbon exuded by algae, and in return, provide vitamins and/or recycled nutrients that are required for algal growth (Kottmeier et al. 1987, Archer et al. 1996, Taylor & Sullivan 2008). Finally, exuded organic carbon may also be an end product of overflow metabolism, whereby cells release the carbon derived from primary production that is excessive to their growth requirements (Fogg 1983), as has been previously reported for planktonic and benthic diatoms (e.g. Myklestad et al. 1989, Staats et al. 2000, Bucciarelli & Sunda 2003).

The identification of specific mechanisms behind exudation of organic carbon by ice algae has been impeded by the complexity and confinement of the sea-ice habitat. Laboratory-based studies of ice-associated diatoms have shown that both exudation rates and the molecular composition of organic carbon vary in response to physicochemical conditions, algal growth phase, and photosynthetic activity (Aslam et al. 2012, Ugalde et al. 2013). A significant component of sea-ice dissolved organic carbon (DOC) contains carbohydrates (total carbohydrates, TCHO) comprising mono- (CHO$_{Mono}$) and polysaccharides (CHO$_{Poly}$; Herborg et al. 2001), which vary in complexity from short-chain (<10 monomers) and long-chain (from 40 up to many 1000s of monomers) molecules to high molecular weight compounds (Decho 2000, Bellinger et al. 2005, Underwood et al. 2010). The adhesive properties of exuded carbohydrates have the poten-

tial to coagulate into gels and to bind microbial aggregates, which, under natural conditions, can be modified through biotic (e.g. microbial modification) and abiotic (e.g. hydrolysis, photolysis) catalysts (Underwood et al. 2010). The non-carbohydrate component of DOC may include an array of proteins, lipids, and free DNA (Hoagland et al. 1993, Underwood & Paterson 2003, Abdullahi et al. 2006).

Substantial concentrations of particulate organic carbon (POC) and DOC have been measured in most types of sea ice. Several studies have reported large variability in the distribution and composition of DOC, possibly due in part to strong spatial (vertical and horizontal) and temporal gradients in sea ice and brine physicochemistry (Underwood et al. 2010, Juhl et al. 2011, Krembs et al. 2011, Aslam et al. 2012). Contrary to earlier laboratory-based studies (e.g. Krembs et al. 2011, Aslam et al. 2012), the high spatial heterogeneity of extracellular organic carbon composition and distribution in Antarctic sea ice showed no correlation with temperature or salinity gradients (Underwood et al. 2010). However, from data collated from both poles, heterogenic extracellular organic carbon concentrations showed robust relationships with algal biomass gradients (Underwood et al. 2013). The development of these gradients is dependent on the physical properties of the ice, which can restrict the exchange of liquid between brine channels and underlying sea water (Gleitz et al. 1995, Papadimitriou et al. 2007, Meiners et al. 2009). A theoretical threshold of 5% brine volume fraction (V_b/V; i.e. the relative contribution of brine volume to total ice volume) may inhibit brine percolation in columnar ice (Golden et al. 1998, 2007, Vancoppenolle et al. 2010). Early spring sea ice is generally characterised by strong vertical gradients in temperature, brine salinity, and overall lower brine volumes when compared with later in the season (Eicken 1992), and this affects sea-ice permeability, biological activity and biogeochemistry (Gleitz et al. 1995, Papadimitriou et al. 2007, Meiners et al. 2009).

This study assesses the dynamics of extracellular organic carbon and algal photophysiology of an Antarctic fast-ice bottom algal community. The concentration of DOC and the relative contribution of total carbohydrates (TCHO—the sum of CHO$_{Mono}$ and CHO$_{Poly}$) was documented for discrete sections of sea ice over a period of 2 wk during the spring–summer transition. This study also provides a description of the microbial community (algal biomass and species composition, maximum quantum photosynthetic yield [F_v/F_m], bacterial abundance, POC and particulate organic nitrogen [PON], partic-

ulate carbon isotopic composition [$\delta^{13}C$]) and brine physicochemistry (V_b/V, ice temperature, bulk ice and brine salinity). It was hypothesised that DOC concentrations and the relative contribution of TCHO would increase with a substantial rise in seasonal algal biomass and photosynthetic activity, influenced by changes in sea-ice physical and chemical parameters.

MATERIALS AND METHODS

Site description and sampling regime

Samples were collected in the vicinity of Turtle Rock (77° 44′ S, 166° 46′ E) in McMurdo Sound, Antarctica, between 16 November and 2 December 2011. A 30 m^2 area was sampled 3 times over a period of 2 wk. On each sampling day, 3 replicate parallel transects each constituting 4 bottom-ice cores (12 cores total) were extracted using a Kovacs ice corer (13 cm internal diameter). To avoid light shock, cores were stored in clean black plastic tubing for transport to the field camp. Two additional cores were collected for a temperature and salinity profile and qualitative Alcian Blue imagery following a modified protocol of Juhl et al. (2011) (Fig. 1).

The transect ice cores were subsequently sliced into discrete sections in a dark room using a purpose-built support frame to allow for accurate and repeatable sectioning. Nine sections were taken from the base of each core: 5 × 1 cm thick sections from 1 to 5 cm; 3 × 2 cm thick sections from 5 to 11 cm; and 1 ×
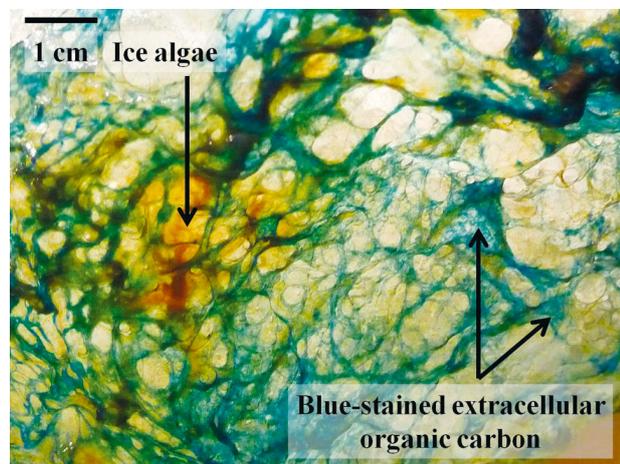

Fig. 1. The bottom of a melting sea-ice core on Day 14 shows ice-associated algae (brown) and extracellular organic carbon (blue; stained with Alcian Blue dye). Image: Sarah C. Ugalde

5 cm thick section from 11 to 16 cm. Corresponding sections from the 4 ice cores of each replicate transect were combined and then melted over a 12 h period at 4°C with the addition of 0.22 µm filtered sea water (200 ml of filtered sea water added per cm of ice-core section) in polypropylene containers that had been rinsed thoroughly with Milli-Q water and autoclaved. The addition of filtered sea water was used to minimise changes in organic carbon exudation as a response to osmotic and temperature stress (Garrison & Buck 1986, Ryan et al. 2004). All particulate analyses were corrected for dilution factors. The dissolved carbon analyses were corrected for the added 0.22 µm filtered sea water, which was collected, filtered, and cooled prior to sampling each day (Riedel et al. 2006). Filtered sea water contained DOC (100 ± 10.14 [SE], 100.83 ± 9.51, and 102.50 ± 14.13 µmol C l^{-1} for initial, 7 d, and 14 d, respectively), CHO_{Mono} (1.63 ± 0.23, 1.82 ± 0.47, and 2.75 ± 0.94 µmol C l^{-1} for initial, 7 d, and 14 d, respectively), and CHO_{Poly} (5.73 ± 0.83, 5.21 ± 1.05, and 6.54 ± 0.94 µmol C l^{-1} for initial, 7 d ,and 14 d, respectively).

Physicochemical profiles and ice-core imagery

Two additional ice cores were extracted on each sampling day: a full-length core for ice temperature and salinity profiles, and a 30 cm bottom-ice section for visualising extracellular organic carbon. Ice temperature was recorded immediately following core extraction. Holes to the centre of the core were produced with a battery-operated hand drill, and a thermometer probe (Hanna HI93510) was inserted into each hole and the temperature was recorded once stabilised. The temperature cores were then transported back to the field camp and sectioned for direct melting in polypropylene containers that had been rinsed thoroughly with Milli-Q water. Once melted, bulk ice salinity was measured with a digital sea water refractometer (Hanna HI96822). Brine salinity (S_b) was estimated from the *in situ* ice-temperature measurements (t) as $S_b = 1000 \times (1 - 54.11/t)^{-1}$ (Petrich & Eicken 2010). The brine-volume fraction, expressed as relative fraction of brine to ice volume (V_b/V), was calculated from the measured ice temperatures and bulk salinities using the equations in Cox & Weeks (1983) and Leppäranta & Manninen (1988).

For visualising extracellular organic carbon, the bottom 30 cm of the core was kept cool to prevent ice melt and placed in a light-protected container with Alcian Blue solution diluted with 0.22 µm filtered sea

water for 12 h, following the protocol of Juhl et al. (2011). The stained core was then suspended from a horizontal beam and left to slowly melt at approximately 4°C (Fig. 1).

Maximum quantum yield (F_v/F_m)

Maximum quantum yield (F_v/F_m) was measured using a pulse amplitude modulated fluorometer (WaterPAM, Waltz). Ice shavings from the 4 cores of each replicate transect were collected during sectioning, and immediately measured with the addition of filtered sea water according to McMinn et al. (2010). Instrument gain settings were between 4 and 17.

Algal biomass and bacterial abundance

For each core section, algal species composition, abundance, and biovolume were determined from subsamples of 30 ml, preserved with glutaraldehyde (0.2% final concentration). For species counts, a subsample of 2 to 20 ml was allowed to settle for >6 h in a 37 mm diameter Utermöhl chamber, and counted at a magnification of 400× using a Zeiss Axiovert inverted microscope at the Australian Antarctic Division (Tasmania). Both live and dead cells were counted (e.g. Oppenheim & Ellis-Evans 1989). Dead cells were those with no observable cell contents. Counts were conducted over random fields of view, until at least 400 (mean ± SE: 742 ± 55) cells had been counted.

Subsamples of 10 ml, used for measuring total brine biovolume, were pre-filtered through 50 µm mesh disks in a 47 mm filter holder, fixed to a sterile syringe. From each sample, the biovolume of particles measuring 3.74 to 60.00 µm in diameter was calculated from 3 × 2 ml subsamples using a Beckman Coulter Counter (Multisizer 3). Biovolume is expressed as total brine biovolume, by correcting for the ice dilution factor.

Samples for chl *a* analysis (30 to 50 ml) were filtered onto 47 mm GF/F (Whatman) filters and stored at −20°C. Chl *a* was extracted from each filter within 48 h of the initial freezing using high-performance liquid chromatography-grade methanol (20 h in the dark at 4°C). Chl *a* concentrations were determined fluorometrically using a Turner Design Model 10-AU digital fluorometer, calibrated against chl *a* standards (Sigma Chemicals; Holm-Hansen & Riemann 1978).

Bacterial abundance samples (10 ml) were preserved with glutaraldehyde (2% final concentration) and stored at −20°C for later analysis at the Australian Antarctic Division (Tasmania). Thawed samples of 500 µl were stained with Xul SYBR Green I nucleic acid gel (Molecular Probes) and incubated in the dark at room temperate for 20 min (Thomson et al. 2010). Cells were then counted using a Becton Dickinson FACScan flow cytometer, according to the protocol of Thomson et al. (2010). Green reference beads (Molecular Probes) were added to each sample prior to staining. Manual gating was used to discriminate between bacterial cells of high (HNA) and low (LNA) nucleic acid content according to Bouvier et al. (2007).

Particulate organic carbon and nitrogen and carbon isotopes

Particulate organic carbon (POC) and nitrogen (PON) samples (15 to 400 ml) were filtered onto pre-combusted (12 h at 450°C) 25 mm diameter quartz filters (Sartorius) and stored at −80°C. Thawed samples and blank filters were acidified with fuming 37% HCl in a bell apparatus for 24 h and dried in a clean oven (15 h at 60°C). Filters were pressed into 5 × 9 mm pre-combusted silver capsules (SerCon) and analysed at the Central Science Laboratory (University of Tasmania) by combustion in an oxygen-enriched helium atmosphere using a Haereus CHN-O-Rapid analyser.

Carbon isotopic composition of ^{13}C relative to ^{12}C ($\delta^{13}C$) samples (15 to 500 ml) were filtered onto 25 mm diameter pre-combusted quartz filters (Sartorius) and prepared as above. Analysis was performed by continuous flow mass spectrometry with a Fisons 1500 elemental analyser coupled to a Finigan MAT Delta S mass spectrometer. Calibration was made by comparison with 15 µg aliquots of NBS22 oil ($\delta^{13}C$ = −29.7; NIST), which was run before and after the sea-ice samples.

Extracellular organic carbon

DOC and CHO samples (100 to 600 ml) were filtered through pre-combusted 45 mm GF/F filters (Whatman) under gentle vacuum pressure (<200 mm Hg) and stored at −20°C for later analysis at the University of Tasmania and the Australian Antarctic Division (Tasmania). Samples were thawed, and DOC subsamples (20 to 30 ml) were decanted into

clean 40 ml glass vials (Shimadzu; acid washed overnight and rinsed 3 times with Milli-Q water, followed by overnight pre-combustion at 500°C). The concentration of DOC in each sample was measured using a total organic carbon analyser (Shimadzu, L-Series), as described by Qian & Mopper (1996). DOC concentrations are expressed as mmol C l^{-1}, and have been normalised to chl a concentrations (mg C [mg chl a]$^{-1}$).

Carbohydrate composition (CHO$_{Mono}$ and CHO$_{Poly}$) was determined using the 2,4,6-tri pyridyl-s-triazine (TPTZ) spectroscopic method developed by Myklestad (1977) and modified by Hung & Santschi (2001). Prior to use, all glassware was acid washed overnight and rinsed 3 times with Milli-Q water, followed by pre-combustion (12 h at 500°C). The carbohydrate concentration was measured against Milli-Q water using a Beckman spectrophotometer (DU640) and fitted to a D-glucose calibration curve. Due to the high light sensitivity of the analytical reagents, reactions were carried out either in the dark or with minimal red light (van Oijen et al. 2004). Carbohydrate concentrations are expressed as µmol C l^{-1}, and have been normalised to chl a concentrations (mg C [mg chl a]$^{-1}$).

Statistical analysis

All statistical analyses were performed using SAS (v.9.2). Only non-parametric statistics (Mann-Whitney U-test, p) were used to determine the statistical significance of vertical and temporal variations in extracellular organic and microbial physiological parameters, given the high variability and non-normal distribution of the data. Correlations were examined by Pearson's correlation analyses.

RESULTS

Physicochemical profiles

Fast-ice thickness was 1.90, 1.89, and 1.87 m for the initial, 7 d, and 14 d sampling dates, respectively. The temperature at the ice–water interface was −1.7, −1.1, and −1.3°C, for initial, 7 d, and 14 d, respectively (Fig. 2A). Sea-ice brine salinities ranged from 20 to 77 (mean: 37 ± 2 [SE]) and showed profiles with the minima towards the interior of the ice. Ice bulk salinities showed a reduction from the ice–water interface, with 14 d measurements beyond 4 cm from the ice–water interface not determined due to a sensor failure (Fig. 2B). Calculated brine volume fraction (mean: 22%; range: 9 to 52%) decreased exponentially from the ice–water interface for all sampling dates; 38, 52, and 43% for initial, 7 d, and 14 d, respectively (Fig. 2C).

Algal biomass and photophysiology

Profiles of chl a concentrations (mean: 97.99 µg l^{-1}; range: 0.26 to 635.16 µg l^{-1}) and F_v/F_m (mean: 0.16; range: 0.05 to 0.45) varied vertically and temporally (p < 0.001; Fig. 3A,B). The vertical profiles of chl a concentrations showed an exponential decrease from the ice–water interface, although they did not sig-
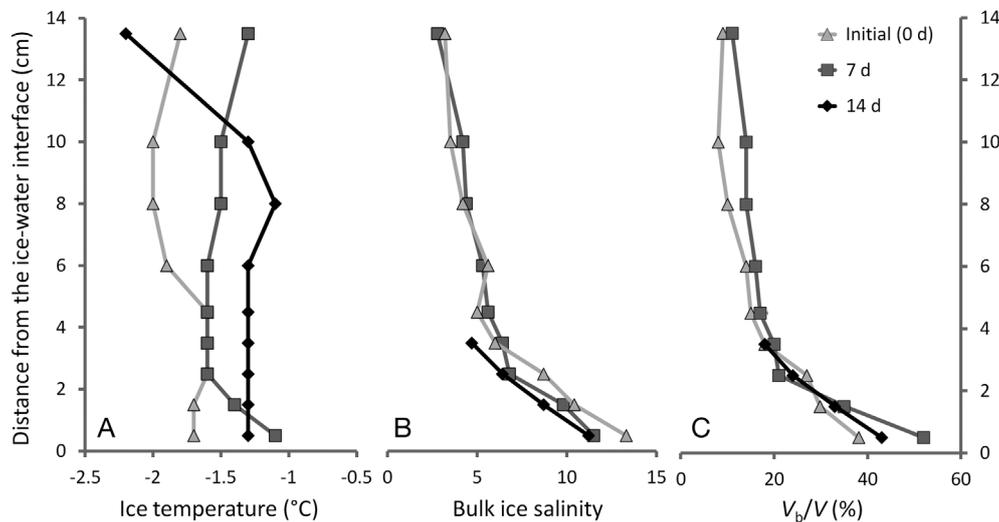

Fig. 2. Vertical and temporal profiles of (A) ice temperature, (B) ice bulk salinity, and (C) calculated brine volume (V_b/V) percentage
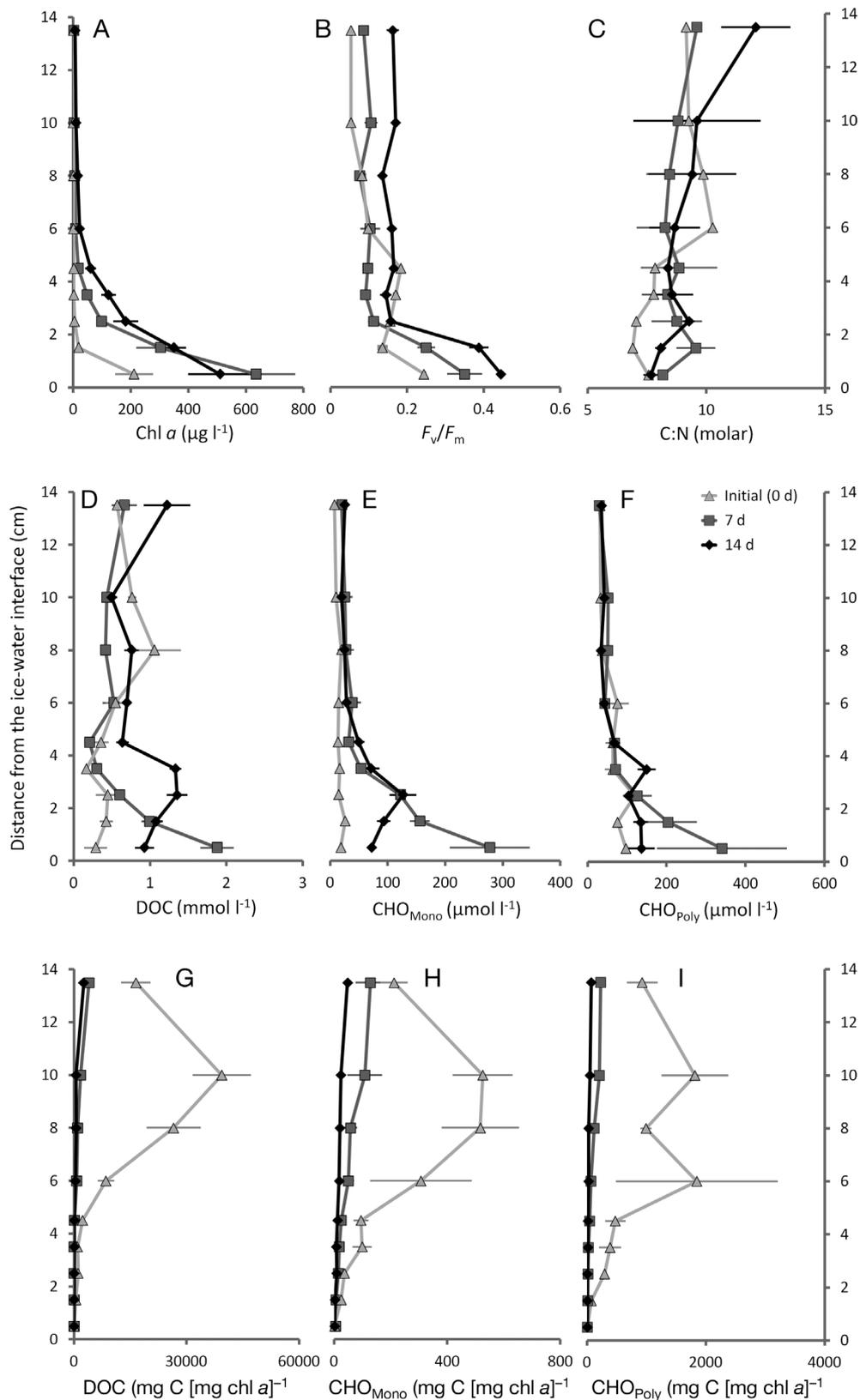
Fig. 3. Vertical and temporal profiles of (A) chlorophyll *a* (chl *a*), (B) maximum photosynthetic yield (F_v/F_m), (C) particulate organic carbon (POC):particulate organic nitrogen (PON) ratio (C:N), (D) dissolved organic carbon (DOC), (E) dissolved monosaccharides (CHO_{Mono}), (F) dissolved polysaccharides (CHO_{Poly}), and extracellular carbon components — (G) DOC, (H) CHO_{Mono} and (I) CHO_{Poly} — normalised to chl *a* concentrations. Error bars = ± SE

nificantly vary between 7 and 14 d. Initial chl *a* concentration at the ice–water interface was 211.80 ± 65.73 µg l^{-1}, reducing by 97% within the first vertical 2 cm. At 7 d, chl *a* concentrations at the ice–water interface (635.16 ± 136.51 µg l^{-1}) reduced by 91% within the first vertical 4 cm, thereafter remaining <20 µg l^{-1}. At 14 d, chl *a* concentrations also reduced, declining by 92% within 7 cm from the ice–water interface (Fig. 3A). For each sampling date, F_v/F_m values showed an exponential decrease from the ice–water interface; with maximum values of 0.24 ± 0.01, 0.35 ± 0.05, and 0.45 ± 0.01, for initial, 7 d, and 14 d, respectively (Fig. 3B).

Molar POC to PON (C:N) ratios of melted ice cores are shown in Fig. 3C. Means for the combined dataset were 8.40, 8.75, and 9.08 for initial, 7 d, and 14 d, respectively (range: 6.89 to 12.08). The high standard errors between replicate cores resulted in no significant vertical or temporal variation.

The vertical profiles of initial δ^{13}C were relatively constant (range: −23.3 to −25.95), with one excep-

tion at 9 to 11 cm above the ice–water interface (Table 1). δ^{13}C values of 7 and 14 d increased from the ice–water interface towards the interior of the sea ice. δ^{13}C values at 7 d then declined from 2 to 3 cm above the ice–water interface to −21.0 at 11 to 16 cm above (Table 1). Similarly, 14 d δ^{13}C values declined between 2 to 7 cm above the ice–water interface, followed by a steady increase between 7 and 16 cm (Table 1). δ^{13}C values were positively correlated with C:N ratios (Pearson correlation coefficient (r_p) = 0.559, significance level (p) = 0.002, sample size (n) = 81), and CHO$_{Mono}$ (r_p = 0.522, p = 0.002, n = 81).

Microalgal taxa and bacterial abundance

Microscopic analysis showed that the bottom-ice algal community was dominated by *Entomoneis kjellmanni*, *Nitzschia stellata*, *Berkeleya adeliense*, *Mangulinea* spp., and *Fragilariopsis* spp. (Table 1),

Table 1. Temporal changes in particulate carbon isotopic composition (δ^{13}C), algal cell abundance, ratio of live:dead algal cells (live algal abundance %), total brine biovolume (3.74 to 60.00 µm diameter), and relative contribution of dominant algal groups to cell abundance

	Time	Distance from ice–water interface (cm)								
		0–1	1–2	2–3	3–4	4–5	5–7	7–9	9–11	11–16
δ^{13}C	Initial	−23.4	−24.7	−24.7	−25.1	−25.6	−24.6	−26.0	−21.3	−24.4
	7 d	−20.6	−16.1	−14.5	−15.9	−17.6	−17.9	−19.3	−20.4	−21.0
	14 d	−24.7	−19.8	−15.9	−16.6	−17.4	−19.6	−24.4	−23.4	−19.0
Algal cell abundance	Initial	33.8	3.4	2.2	1.2	1.6	1.3	0.7	0.7	0.3
(×10^3 cells ml^{-1})	7 d	91.9	19.9	15.9	9.6	3.9	3.3	2.2	1.6	1.0
	14 d	72.2	65.7	12.8	14.4	4.1	8.0	3.8	1.9	1.2
Live algal abundance (%)	Initial	98.0	97.1	76.2	90.0	94.2	89.0	93.0	69.3	83.4
	7 d	98.0	97.4	95.3	94.6	94.4	94.8	90.9	85.3	91.1
	14 d	94.1	95.1	98.3	98.1	97.8	87.7	94.3	94.9	90.4
Total brine biovolume	Initial	41.6	4.4	1.3	0.9	0.9	0.8	0.6	0.5	0.4
(×10^4 µm^3 ml^{-1})	7 d	113.3	33.4	26.5	18.0	3.6	4.6	3.1	2.9	9.2
	14 d	39.1	38.9	44.5	17.7	4.7	4.3	4.0	2.5	2.2
Relative contribution (%) of:										
Entomoneis kjellmanni	Initial	18.6	0.4	6.7	7.2	3.3	5.2	3.2	0.0	0.0
	7 d	46.4	4.3	4.0	3.5	1.4	0.6	0.7	1.2	1.4
	14 d	27.8	40.3	3.3	1.7	2.1	11.2	3.6	1.7	1.9
Nitzschia stellata	Initial	37.8	6.5	7.2	10.2	1.9	10.7	4.8	4.2	0.6
	7 d	8.4	50.8	32.5	22.9	17.5	8.3	8.5	3.0	4.1
	14 d	2.2	5.4	45.3	47.8	22.4	24.0	6.5	17.6	17.4
Berkeleya adeliense	Initial	6.1	0.7	5.4	2.2	1.3	1.4	12.3	2.8	1.1
	7 d	10.3	15.6	20.6	25.2	22.4	7.0	12.0	20.0	7.1
	14 d	1.7	3.4	25.5	21.9	14.5	24.3	7.2	56.4	12.1
Mangulinea spp.	Initial	7.9	6.2	10.9	11.9	5.6	2.8	7.6	0.7	1.6
	7 d	2.8	8.0	7.4	6.1	10.7	11.2	8.4	6.6	2.4
	14 d	1.0	5.6	12.3	10.7	8.7	13.5	4.1	1.7	1.1
Fragilariopsis spp.	Initial	11.5	7.6	5.9	5.4	4.1	6.8	2.5	0.0	0.8
	7 d	11.1	4.7	3.5	1.9	2.0	0.6	2.8	1.3	0.5
	14 d	9.8	0.4	0.7	0.8	3.7	2.0	0.6	2.0	1.7

with other notable taxa including *Chaetoceros* spp., *Pleurosigma* spp., *Pinnularia quadreata*, and *Porosira glacialis.* Vertical and temporal cell abundance measurements varied significantly (p < 0.001) and decreased exponentially from the ice–water interface. Algal cell abundance decreased by approximately 99% at 11 to 16 cm above the ice–water interface for all sampling dates (Table 1). The proportion of live algal cells relative to the total abundance (i.e. % live cells) ranged from 69.3 to 93.3% (p < 0.0001; mean: 91.8%; Table 1). For initial and 7 d, the % live cells were highest at the ice–water interface (98.0%; Table 1), strongly declining with distance above this level. For 14 d, the % live cells showed a similar pattern to chl *a* concentrations, and was highest at 2 to 3 cm above the ice–water interface (98.3%; Table 1).

Brine biovolumes are shown in Table 1, and ranged from 0.4×10^4 to 113.3×10^4 µm³ ml⁻¹ (p < 0.0001; mean: 15.7×10^4 µm³ ml⁻¹). Total brine biovolume measurements at the ice–water interface for initial (41.6×10^4 µm³ ml⁻¹) and 7 d (113.3×10^4 µm³ ml⁻¹) declined by 98 and 76% at 11 to 16 cm above, respectively. 14 d total brine biovolume measurements were highest at 2 to 3 cm above the ice–water interface (44.5×10^4 µm³ ml⁻¹), thereafter reducing by 91% at 11 to 16 cm (Table 1). Total brine biovolume was significantly positively correlated with chl *a*, POC, and maximum quantum yield (chl *a*: $r_p = 0.721$, p < 0.001, n = 27; POC: $r_p = 0.834$, p < 0.001, n = 27; F_v/F_v: $r_p = 0.750$, p < 0.001, n = 27) and extracellular organic carbon concentrations (DOC: $r_p = 0.811$, p < 0.001, n = 27; CHO$_{Mono}$: $r_p = 0.745$, p < 0.001, n = 27; CHO$_{Poly}$: $r_p = 0.627$, p < 0.001, n = 27).

Total bacterial abundance fractionated into HNA and LNA content varied between sections and ranged from 0.54×10^5 to 28.90×10^5 cells ml⁻¹ (mean: 6.05×10^5 cells ml⁻¹) and 0.49×10^5 to 48.47×10^5 cells ml⁻¹ (mean: 16.22×10^5 cells ml⁻¹), respectively. Initial HNA and LNA bacterial abundance was highest at the ice–water interface (mean: $28.90 \times 10^5 \pm 28.73 \times 10^5$ [SE] and $20.56 \times 10^5 \pm 19.51 \times 10^5$ cells ml⁻¹, respectively) reducing by 94 and 91% within 4 cm from the ice–water interface. HNA bacterial abundance for 7 d (mean: $6.20 \times 10^5 \pm 1.39 \times 10^5$ cells ml⁻¹) and 14 d (mean: $6.69 \times 10^5 \pm 0.96 \times 10^5$ cells ml⁻¹) were reduced by 81 and 36% at 4 to 5 cm and 6 to 7 cm above the ice–water interface, respectively (Fig. 4A). LNA bacterial abundance for 7 d (mean: $19.65 \times 10^5 \pm 16.01 \times 10^5$ cells ml⁻¹) and 14 d ($25.19 \times 10^5 \pm 17.63 \times 10^5$ cells ml⁻¹) showed high standard errors, increasing by 72 and 52% at 3 to 4 cm above the ice–water interface, respectively (Fig.

4B). HNA bacterial abundance was correlated with ice temperature ($r_p = 0.503$, p = 0.010, n = 27) and chl *a* concentration ($r_p = 0.363$, p = 0.001, n = 81). LNA bacterial abundance was positively correlated with C:N ratio ($r_p = 0.293$, p = 0.012, n = 81).

Extracellular organic carbon components

Vertical and temporal measurements of DOC concentrations showed significant variation (p < 0.005; mean: 0.71 ± 0.08 mmol C l⁻¹), with each sampling date showing dissimilar vertical profiles (Fig. 3D). Initial DOC concentrations ranged between 0.16 and 1.06 mmol C l⁻¹ (mean: 0.51 ± 0.09 [SE] mmol C l⁻¹), and showed no significant vertical variation. 7 d DOC concentrations showed a significant decline, reducing by 89% at 4 to 5 cm above the ice–water interface (p < 0.005; mean: 0.67 ± 0.17 mmol C l⁻¹; range: 0.21 to 1.88 mmol C l⁻¹). 14 d DOC concentrations reached 1.35 ± 0.14 mmol C l⁻¹ at 2 to 3 cm above the ice–water interface (p < 0.005; mean: 0.94 ± 0.11 mmol C l⁻¹), thereafter declining by 79% at 11 to 16 cm above (Fig. 3D). DOC concentrations were correlated with chl *a* concentrations ($r_p = 0.649$, p < 0.001, n = 81), F_v/F_m ($r_p = 0.574$, p < 0.001, n = 81), and dissolved carbohydrates (CHO$_{Mono}$: $r_p = 0.766$, p < 0.001, n = 81; CHO$_{Poly}$: $r_p = 0.738$, p < 0.001, n = 81).

Values of CHO$_{Mono}$ ranged between 7 and 278 µmol C l⁻¹ (mean: 52 ± 11 [SE] µmol C l⁻¹), and CHO$_{Poly}$ ranged between 30 and 341 µmol C l⁻¹ (mean: 86 ± 13 µmol C l⁻¹; Fig. 3E,F). Initial CHO$_{Mono}$ values were low (range: 7 to 26 µmol C l⁻¹; mean: 16 ± 2 µmol C l⁻¹) and were highest at 1 to 2 cm above the ice–water interface (Fig. 3E). CHO$_{Poly}$ initial values ranged between 31 and 120 µmol C l⁻¹ (mean: 67 ± 10 µmol C l⁻¹), and were highest at 2 to 3 cm above the ice–water interface (Fig. 3F). 7 d dissolved carbohydrates were highest at the ice–water interface; CHO$_{Mono}$ (range: 20 to 278 µmol C l⁻¹; mean: 84 ± 29 µmol C l⁻¹) and CHO$_{Poly}$ (range: 30 to 341 µmol C l⁻¹; mean: 110 ± 34 µmol C l⁻¹) reduced by 92 and 91% at 11 to 16 cm above, respectively. 14 d CHO$_{Mono}$ values were highest at 2 to 3 cm above the ice–water interface (range: 20 to 127 µmol C l⁻¹; mean: 57 ± 12 µmol C l⁻¹), reducing by 91% at 11 to 16 cm above (CHO$_{Poly}$ range: 34 to 150 µmol C l⁻¹; mean: 83 ± 16 µmol C l⁻¹). Concentrations of CHO$_{Mono}$ and CHO$_{Poly}$ both showed a correlation with ice temperature ($r_p = 0.408$, p = 0.043, n = 27), chl *a* concentrations ($r_p = 0.74$ and 0.471, respectively, p < 0.001, n = 81) and F_v/F_m ($r_p = 0.449$ and 0.516, respectively, p < 0.001, n = 81).
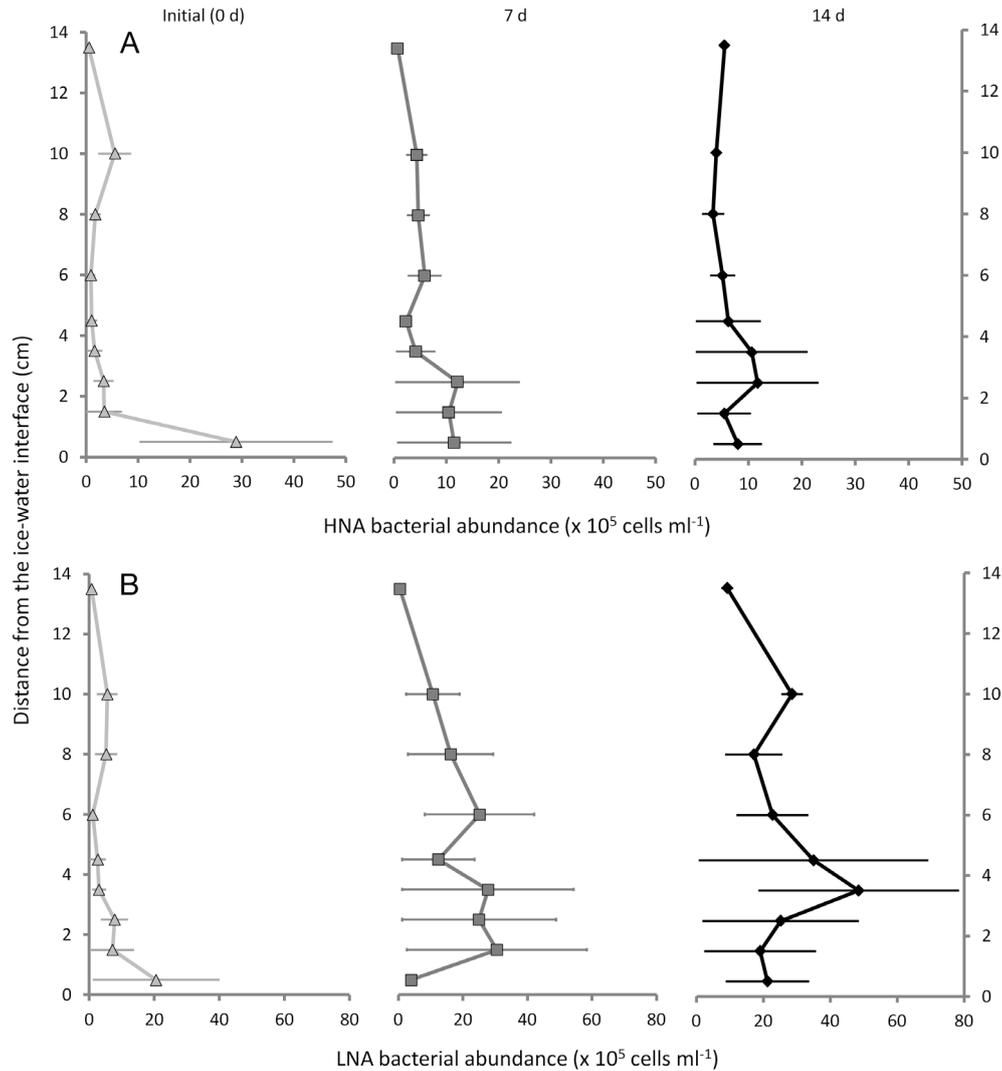
Fig. 4. Vertical and temporal profiles of (A) high nucleic acid (HNA) bacterial cell abundance and (B) low nucleic acid (LNA) bacterial abundance. Error bars = ± SE

Biomass-normalised extracellular organic carbon components

Chl *a*-normalised DOC concentrations showed significant vertical and temporal variation (p < 0.005; mean: 4019 ± 1772 [SE] mg C [mg chl *a*]$^{-1}$; range: 23 to 39 401 mg C [mg chl *a*]$^{-1}$; Fig. 3G). Chl *a*-normalised DOC was lowest at the ice–water interface: 33 ± 27, 39 ± 9, and 23 ± 3 mg C (mg chl *a*)$^{-1}$, for initial, 7 d, and 14 d, respectively (Fig. 3G). Initial chl *a*-normalised DOC concentrations vertically increased to reach a maxima of 39 401 ± 7736 mg C (mg chl *a*)$^{-1}$ at 9 to 11 cm above the ice–water interface. 7 d and 14 d chl *a*-normalised DOC also strongly increased from the ice–water interface (p < 0.005), to reach 2809 ± 251 and 2539 ± 1796 mg C [mg chl *a*]$^{-1}$ at 11 to 16 cm above, respectively (Fig. 3G).

Chl *a*-normalised CHO$_{Mono}$ concentrations were low at the ice–water interface: 1.6 ± 1.0, 5.2 ± 0.2, and 2.0 ± 0.8 mg C (mg chl *a*)$^{-1}$ for initial, 7 d, and 14 d, respectively (Fig. 3H). Initial chl *a*-normalised CHO$_{Mono}$ concentrations (range: 1.6 to 525.5 mg C [mg chl *a*]$^{-1}$; mean: 202.1 ± 67.7 [SE] mg C [mg chl *a*]$^{-1}$) were highest at 7 to 9 cm above the ice–water interface, and CHO$_{Poly}$ concentrations (range: 3.7 to 1849.0 mg C [mg chl *a*]$^{-1}$; mean: 287.9 ± 99.3 mg C [mg chl *a*]$^{-1}$) were highest at 5 to 7 cm above the ice–water interface (Fig. 3H,I). In comparison, chl *a*-normalised dissolved carbohydrates for both 7 d (CHO$_{Mono}$ range: 5.2 to 128.0 mg C [mg chl *a*]$^{-1}$; mean: 46.2 ± 15.0 mg C [mg chl *a*]$^{-1}$; CHO$_{Poly}$ range: 7.7 to 208.3 mg C [mg chl *a*]$^{-1}$; mean: 80.7 ± 28.7 mg C [mg chl *a*]$^{-1}$) and 14 d (CHO$_{Mono}$ range: 2.0 to 47.7 mg C [mg chl *a*]$^{-1}$; mean: 16.1 ± 4.7 mg C [mg
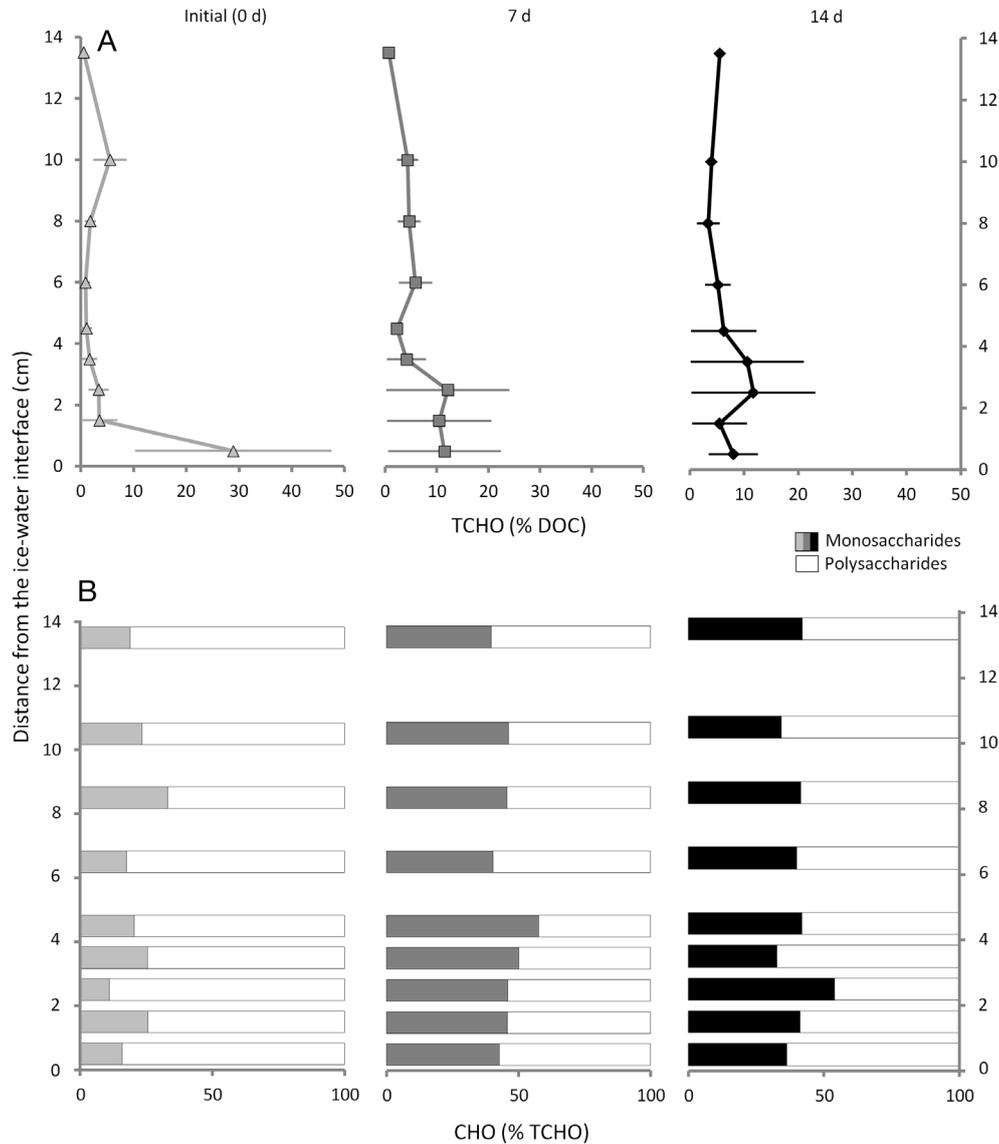
Fig. 5. Temporal and vertical profiles of dissolved organic carbon (DOC) composition. (A) Relative contribution of total carbohydrates (TCHO) to DOC. (B) Relative contribution of dissolved monosaccharides (CHO_{Mono}) and polysaccharides (CHO_{Poly}) to TCHO. Error bars = ± SE

chl $a]^{-1}$; CHO_{Poly} range: 3.7 to 71.2 mg C [mg chl $a]^{-1}$; mean: 24.4 ± 7.5 mg C [mg chl $a]^{-1}$) were low (Fig. 3H,I).

DOC composition

The relative contribution of TCHO to DOC showed significant spatial and temporal variation ($p < 0.005$; mean: 24.9 ± 3.4 [SE] %; range: 5.6 to 76.3%; Fig. 5A). This portion of TCHO had high CHO_{Poly} contributions for initial measurements (mean: 78.8 ± 2.2%; range: 66.9 to 89.06%; Fig. 5B). At 7 d, the relative proportion of CHO_{Poly} to TCHO reached a maxima at

9 to 11 cm above the ice−water interface, ranging between 49.3 and 70.4% (mean: 59.22 ± 2.62%; Fig. 5B). At 14 d, the relative proportion of CHO_{Poly} to TCHO increased from the ice−water interface to reach 67.3 ± 8.2% at 2 to 3 cm above, ranging between 46.01 and 67.3% (mean: 59.6 ± 3.0%; Fig. 5B).

DISCUSSION

Seasonal changes in sea-ice physical parameters create strong physicochemical gradients that affect biological activity and biogeochemistry (Gleitz et al. 1995, Papadimitriou et al. 2007, Vancoppenolle et al.

2010, 2013). At McMurdo Sound in November to December 2011, the calculated V_b/V fraction was well above the theoretical threshold of 5% (Golden et al. 1998, 2007; mean range: 28 to 32% at 0 to 4 cm above the ice–water interface for sampling dates) and is interpreted as an open brine channel network (i.e. ice melting), allowing for increased capacity for fluid transport across the ice–water interface by mixing nutrient-poor brine with comparatively fresh, nutrient-rich sea water (Vancoppenolle et al. 2010). This fluid transport potential can be impeded by the development of brine salinity stratification caused by melting sea ice during warmer temperatures. Nonetheless, the observed increase in algal biomass (as indicated by chl *a* concentration and algal cell abundance) increased to within expected ranges for a bottom-ice community at the ice–water interface (e.g. McMinn et al. 1999, Ryan et al. 2006). The taxonomic composition was comparable to previous studies in this area, although the relative abundance of the major taxa varied considerably over the 2 wk period. At Cape Evans over the spring–summer transition, McMinn et al. (2000) reported that *Nitzschia stellata* dominated the algal community (up to 94% of cells), with *Berkeleya adeliensis*, *Pleurosigma antarctica*, *Entomoneis kjellmannii*, and *N. lecoitei* also present. Fiala et al. (2006) reported *Fragilariopsis*, *Nitzschia*, *Navicular*, and *Pseudonitzschia* were dominant at Adelie Land during April to December, and were influenced by large spatial variability. In the present study, the bottom-ice community was dominated by colony-forming diatoms: *N. stellata* (51% maximum), *E. kjellmannii* (46% maximun), and *B. adeliensis* (56% maximum). These particular species may exude organic carbon for the purpose of cell attachment (Hoagland et al. 1993), and formation of colonies may partly account for the spatial heterogeneity within measured particulate (e.g. C:N, δ^{13}C, chl *a*) and dissolved (e.g. DOC, CHO_{Mono}, CHO_{Poly}) parameters.

The photosynthetic parameter, F_v/F_m, was lower than expected (mean at the ice–water interface = 0.35), which for unstressed marine microalgae is typically 0.65 (Schreiber 2004). McMinn et al. (2003) reported F_v/F_m values of 0.45 ± 0.15 in over 100 dark-adapted samples from Antarctic fast ice. In the Arctic, McMinn & Hegseth (2004) have also reported similar values from apparently healthy sea-ice communities. Therefore, the results herein are consistent with the suggestions that *in situ* ice algal communities have naturally low F_v/F_m values, possibly due to a temperature influence on photosynthetic performance (McMinn et al. 2010). In the present study, the vertical reduction in F_v/F_m values demonstrated a clear coupling with algal biomass, and is interpreted as a consequence of increasing restrictive brine dynamics above the ice–water interface (i.e. V_b/V).

Fast-ice algal communities exhibit a seasonal trend with respect to nutrient stress (Lizotte & Sullivan 1992). Typically, nitrogen limitation is evident when C:N ratios are >7.7 (Redfield et al. 1963). For congelation ice, high ratios have been reported (e.g. Cota & Sullivan (1990): range = 8.8 to 16; Lizotte & Sullivan (1992): range = 7.8 to 14.6). In the present study, although slightly elevated C:N ratios were measured (mean: 8.4, 8.7, and 9.1 for initial, 7 d, and 14 d, respectively), the high spatial heterogeneity suggests skewed abundances of colony-forming cells and/or that cell-associated or colloidal extracellular organic carbon was captured on the filters during sampling. This may have resulted in an overestimation of C:N ratios, and as such, the bottom-ice community is considered to have experienced reduced nutrient availability, but was not necessarily nutrient limited.

Along with nutrient drawdown, bottom-ice assemblages may also be limited by the supply of CO_2 (Riebesell et al. 1993). Any reduction in aqueous CO_2 will be reflected in more positive δ^{13}C values of the algae (Popp et al. 1999). In the present study, the δ^{13}C profiles showed an increase within 3 cm above the ice–water interface for 7 d and 14 d. This trend implies that demand for CO_2 exceeded supply (i.e. drawdown, Kennedy et al. 2002); either the demand for CO_2 is increased due to high algal growth, or alternatively, the supply of CO_2 across the ice–water interface is limited due to restrictive brine dynamics. In the present study, although a combination of both factors is likely, the latter maybe more important as algal growth rates need to be high to influence carbon isotopic composition (McMinn et al. 1999). For example, culture experiments with *Phaeodactylum tricornutum* revealed that growth rates in excess of 0.5 d^{-1} were needed to affect δ^{13}C values (Laws et al. 1997). This rate was not exceeded in the present study, with average ice algal *in situ* net cell growth rate estimates (calculated from changes in algal cell abundance) of 0.19 ± 0.02 (range: 0.12 to 0.30) and 0.05 ± 0.02 (range: −0.03 to 0.17) for initial to 7 d, and 7 to 14 d, respectively. These growth rates are comparable to typical values of 0.1 to 0.2 d^{-1} previously observed in Antarctic fast ice (Palmisano & Sullivan 1983, Sullivan et al. 1985).

The ecological functions of bacterial communities are influenced by their phylogenetic composition, representing a wide range of DNA contents and cell sizes (Bouvier et al. 2007). HNA bacteria are generally larger, more metabolically active, and have

higher growth rates than their LNA counterparts (Lebaron et al. 2002, Servais et al. 2003, Bouvier et al. 2007). In the present study, the HNA bacterial abundance was correlated with chl a concentrations (r_p = 0.363, p = 0.001, n = 81) and ice temperature (r_p = 0.503, p = 0.010, n = 27); LNA bacterial abundance had no such correlation. This may infer a direct association between the HNA bacteria and algal fractions of the community by means of a microbial loop, although this relationship is dependent on microbial composition (Taylor & Sullivan 2008, Martin et al. 2012), or, alternatively, this association may be a consequence of warmer temperatures promoting general microbial growth. The lack of correlation between the bacterial community and exuded organic material is inconsistent with findings from other sea-ice studies (e.g. Meiners et al. 2004), although a complete understanding of microbial and extracellular organic carbon dynamics within the sea-ice ecosystems clearly requires information beyond the use of proxy measurements (Garrison et al. 2005).

The DOC concentrations in the present study are comparable to other sea-ice studies from Antarctic and Arctic regions (Carlson et al. 2000, Herborg et al. 2001, Krembs et al. 2002, Underwood et al. 2010). Compared with marine environments, DOC concentrations were more than 10-fold higher than those measured in surface oceanic water in the circumpolar Southern Ocean (Pakulski & Benner 1994, Kähler et al. 1997, Wedborg et al. 1998, Carlson et al. 2000, Doval et al. 2002, Papadimitriou et al. 2007). Given that the high DOC concentrations were present in the samples that had a high algal biomass (r_p = 0.649, p < 0.001, n = 81), there is clearly a strong link between algal activity and DOC accumulation in Antarctic sea ice, although this is not always the case in other studies (e.g. Herborg et al. 2001). Similarly, carbohydrate accumulation, specifically high-molecular weight carbohydrates expressed as exopolymeric substances, in both sea ice (Krembs & Engel 2001, Riedel et al. 2006, 2008) and sediments (Underwood & Smith 1998) generally show a close correlation with algal biomass. Carbohydrate enrichment has been observed as sea ice ages, and this may be explained by changes in the brine environment, such as nutrient limitation, CO_2 drawdown, and elevated pH (Riedel et al. 2007, Collins et al. 2008, van der Merwe et al. 2009). In contrast, the high DOC concentration towards the ice interior at 14 d may be a due to the high V_b/V values at the ice–water interface, allowing for DOC to be released into the under-ice water prior to, or during, ice-core extraction. Production studies have reported an increase in extracellular organic carbon exudation ac-

companying changes in physiology and growth phase in Antarctic sea-ice algae (Aslam et al. 2012, Ugalde et al. 2013), as also observed in marine diatoms (e.g. Goto et al. 1999, Granum et al. 2002, Underwood et al. 2004). In the present study, chl a-normalised extracellular organic carbon concentrations showed a decrease over the sampling period, which coincided with increases in both F_v/F_m values and V_b/V, indicating an enhanced capacity for nutrient transport from the under-ice realm into the bottom layers of the sea ice. This finding supports the notion that extracellular organic carbon plays an important role in the microbial response to physicochemical conditions (e.g. low temperature, nutrient availability), or possibly represents overflow metabolism.

Overflow metabolism is a well-established mechanism, although it has rarely been applied to polar environments (Myklestad et al. 1989, Waite et al. 1995). Fogg (1983) proposed that the exudation of organic carbon was an end-product of a process whereby photosynthesis takes place more rapidly than is necessary to supply the requirements for growth. Overflow metabolism has since been observed in planktonic and benthic diatoms, and can be stimulated by both nutrient-limiting conditions (e.g. Myklestad et al. 1989, Staats et al. 2000, Bucciarelli & Sunda 2003) and low temperature (e.g. Wolfstein & Stal 2002). For ice-dwelling microbes, an increase in the exudation of organic carbon has been reported at reduced temperatures and nutrient limitation, possibly as a cellular survival mechanism (e.g. Gleitz & Kirst 1991, Krembs & Deming 2008, Krembs et al. 2011, Underwood et al. 2013). However, as low temperatures are usually associated with reduced growth rates, metabolic overflow may better explain this coupling (Mock & Valentin 2004, Krell et al. 2007, Aslam et al. 2012). In the present study, the microbial community was exposed to both reduced, but not limiting, nutrient availability (based on C:N ratios of >7.7) and low temperatures. Therefore, overflow metabolism cannot be excluded as a possible explanation for the observed spatial and temporal trends of chl a-normalised extracellular organic carbon.

The proportion of DOC as TCHO was generally <20%, and this is comparable to previous reported values in Arctic and Antarctic sea water (Pakulski & Benner 1994, Herborg et al. 2001, Engbrodt & Kattner 2005, Myklestad & Børsheim 2007). In Antarctic sea ice, the mean proportion of TCHO to DOC is <35%; however, it ranges from 1 to 99% (Herborg et al. 2001, Thomas et al. 2001). In contrast, Underwood et al. (2010) reported values from melted ice cores of between 30 and 50%, and they considered that this

variation may be due, in part, to differing methods used to isolate and measure carbohydrate concentrations between sea water and ice. For example, the methods used by Underwood et al. (2010) require dialysis to exclude salts from the samples. This resulted in low-molecular weight materials, including carbohydrates <8 KDa, being lost prior to TCHO analysis. In the present study, the methods applied did not require dialysis, but this alone does not explain the difference in TCHO values reported. Rather, the present study suggests that either the carbohydrate fraction of DOC may have been rapidly modified through abiotic (e.g. hydrolysis, photolysis) or biotic (e.g. microbial loop) processes. Alternatively, the bottom-ice microbial assemblages may have invested heavily into non-carbohydrate DOC, consisting of proteins, lipids, and free DNA, possibly also including organic nitrogen-containing carbohydrates (e.g. proteoglycans and amino-sugars; Underwood et al. 2010). The present study supports the need for further research and comparison of methods for the isolation and quantification of extracellular organic carbon components, particularly in the sea-ice habitat.

The present study demonstrates that CHO_{Poly} substantially contributes to TCHO in late spring (mean = 79%), and this contribution rapidly decreases over time (mean = 59%). If extracellular organic carbon provides protection against challenging abiotic conditions (Krembs et al. 2011), then a shift towards molecules with greater structural potential (i.e. polysaccharides) might be expected in addition to any increase in abundance (Krembs & Engel 2001, Krembs & Deming 2008, Underwood et al. 2010). Gleitz & Kirst (1991) reported that interior pack-ice algal assemblages produce approximately 5 times more polysaccharides when compared with infiltration assemblages, possibly due to nutrient limitation in the sea-ice interior. In the present study, the high relative contribution of CHO_{Poly} to TCHO in early season ice indicates that the cells were experiencing adverse abiotic conditions, as was reflected by relatively low F_v/F_m values. This, coupled with lower calculated brine volume in early season ice, suggests a limited capacity for fluid exchange between brine channels and the underlying seawater.

CONCLUSION

The present study provides a detailed description of microalgal physiology and exuded organic carbon dynamics in an Antarctic bottom-ice community, and is the first attempt to describe their successive changes during the spring–summer transition. It was hypothesised that sea-ice algae would increase carbon allocation to extracellular organic components with an increase in algal biomass. This hypothesis was supported with total concentrations of extracellular organic carbon components (DOC and TCHO [sum of CHO_{Mono} and CHO_{Poly}]) increasing during the sampling period. However, extracellular organic carbon concentrations normalised to chl a showed a substantial decrease during the sampling period. This change was associated with improved algal physiology and brine conditions, initiated by an increase in brine volume allowing transport across the ice–water interface. These findings support the theory that exudation of organic carbon by sea-ice algae is associated with adverse brine conditions, either as a direct (in response to reduced temperatures or nutrient availability) or indirect (overflow metabolism or microbial loop) mechanism.

LITERATURE CITED

Abdullahi AS, Underwood GJC, Gretz MR (2006) Extracellular matrix assembly in diatoms (Bacillariophyceae). V. Environmental effects on polysaccharide synthesis in the model diatom, *Phaeodactylum tricornutum*. J Phycol 42:363–378

Archer SD, Leakey RJG, Burkill PH, Sleigh MA, Appleby CJ (1996) Microbial ecology of sea ice at a coastal Antarctic site: community composition, biomass and temporal change. Mar Ecol Prog Ser 135:179–195

Arrigo KR, Mock T, Lizotte MP (2010) Primary producers and sea ice. In: Thomas DN, Dieckmann GS (eds) Sea ice, 2nd edn. Wiley-Blackwell, Oxford, p 283–326

Aslam SN, Cresswell-Maynard T, Thomas DN, Underwood GJC (2012) Production and characterization of the intra- and extracellular carbohydrates and polymeric substances (EPS) of three sea-ice diatom species, and evidence for a cryoprotective role for EPS. J Phycol 48:1494–1509

Azam F, Smith DC, Hollibaugh JT (1991) The role of the microbial loop in Antarctic pelagic ecosystems. Polar Res 10:239–243

Bellinger BJ, Abdullahi AS, Gretz MR, Underwood GJC (2005) Biofilm polymers: relationship between carbohydrate biopolymers from estuarine mudflats and unial-

gal cultures of benthic diatoms. Aquat Microb Ecol 38: 169–180

Bouvier T, Del Giorgio PA, Gasol JM (2007) A comparative study of the cytometric characteristics of high and low nucleic-acid bacterioplankton cells from different aquatic ecosystems. Environ Microbiol 9:2050–2066

Bucciarelli E, Sunda WG (2003) Influence of CO_2, nitrate, phosphate, and silicate limitation on intracellular dimethylsulfoniopropionate in batch cultures of the coastal diatom *Thalassiosira pseudonana*. Limnol Oceanogr 48: 2256–2265

Carlson CA, Hansell DA, Peltzer ET, Smith WO (2000) Stocks and dynamics of dissolved and particulate organic matter in the southern Ross Sea, Antarctica. Deep-Sea Res II 47:3201–3225

Christaki U, Dolan JR, Pelegri S, Rassoulzadegan F (1998) Consumption of picoplankton-size particles by marine ciliates: effects of physiological state of the ciliate and particle quality. Limnol Oceanogr 43:458–464

Collins RE, Carpenter SD, Deming JW (2008) Spatial heterogeneity and temporal dynamics of particles, bacteria and pEPS in Arctic winter sea ice. J Mar Syst 74:902–917

Cota GF, Sullivan CW (1990) Photoadaptation, growth and production of bottom ice algae in the Antarctic. J Phycol 26:399–411

Cox GFN, Weeks WF (1983) Equations for determining the gas and brine volume in sea ice samples. J Glaciol 29: 306–331

Decho AW (2000) Microbial biofilms in intertidal systems: an overview. Cont Shelf Res 20:1257–1273

Doval MD, Alvarez-Salgado XA, Castro CG, Perez FF (2002) Dissolved organic carbon distributions in the Bransfield and Gerlache Straits, Antarctica. Deep-Sea Res II 49: 663–674

Eicken H (1992) The role of sea ice in structuring Antarctic ecosystems. Polar Biol 12:3–13

Engbrodt R, Kattner G (2005) On the biogeochemistry of dissolved carbohydrate in the Greenland Sea (Arctic). Org Geochem 36:937–948

Fiala M, Kuosa H, Kopczyńska EE, Oriol L, Delille D (2006) Spatial and seasonal heterogeneity of sea ice microbial communities in the first-year ice of Terre Adélie area (Antarctica). Aquat Microb Ecol 43:95–106

Fogg GE (1983) The ecological significance of extracellular products of phytoplankton photosynthesis. Bot Mar 26:3–14

Garrison DL, Buck KR (1986) Organism losses during ice melting: a serious bias in sea ice community studies. Polar Biol 6:237–239

Garrison DL, Gibson A, Coale SL, Gowing MM, Okolodkov YB, Fritsen HF, Jefferies MO (2005) Sea ice microbial communities in the Ross Sea: autumn and summer biota. Mar Ecol Prog Ser 300:39–52

Gleitz M, Kirst GO (1991) Photosynthetic-irradiance relationships and carbon metabolism of different ice algal assemblages collected from Weddell Sea pack ice during austral spring (EPOS 1). Polar Biol 11:385–392

Gleitz M, Van der Loeff MR, Thomas DN, Dieckmann GS, Millero FJ (1995) Comparison of summer and winter inorganic carbon, oxygen and nutrient concentrations in Antarctic sea ice brine. Mar Chem 51:81–91

Golden KM, Ackley SF, Lytle VI (1998) The percolation phase transition in sea ice. Science 282:2238–2241

Golden KM, Eicken H, Heaton AL, Miner J, Pringle DJ, Zhu J (2007) Thermal evolution of permeability and microstructure in sea ice. Geophys Res Lett 34, L16501, doi: 10.1029/2007GL030447

Goto N, Kawamura T, Mitamura O, Terai H (1999) Importance of extracellular organic carbon production in the total primary production by tidal-flat diatoms in comparison to phytoplankton. Mar Ecol Prog Ser 190:289–295

Granum E, Kirkvold S, Myklestad SM (2002) Cellular and extracellular production of carbohydrates and amino acids by the marine diatom *Skeletonema costatum*: diel variations and effects on N depletion. Mar Ecol Prog Ser 242:83–94

Herborg LM, Thomas DN, Kennedy H, Haas C, Dieckmann GS (2001) Dissolved carbohydrates in Antarctic sea ice. Antarct Sci 13:119–125

Hoagland KD, Rosowski JR, Gretz MR, Roemer SC (1993) Diatom extracellular polymeric substances: functions, fine structure, chemistry, and physiology. J Phycol 29: 537–566

Holm-Hansen O, Riemann B (1978) Chlorophyll *a* determination: improvements in methodology. Oikos 30:438–447

Hung CC, Santschi PH (2001) Spectrophotometric determination of total uronic acids using cation-exchange separation and pre-concentration by lyophilisation. Anal Chim Acta 427:111–117

Juhl AR, Krembs C, Meiners KM (2011) Seasonal development and differential retention of ice algae and other organic fractions in first-year Arctic sea ice. Mar Ecol Prog Ser 436:1–16

Kähler P, Bjørnsen PK, Lochte K, Anita A (1997) Dissolved organic matter and its utilization by bacteria during spring in the Southern Ocean. Deep-Sea Res II 44: 341–353

Kattner G, Thomas DN, Haas C, Kennedy H, Dieckmann GS (2004) Surface ice and gap layers in Antarctic sea ice: highly productive habitats. Mar Ecol Prog Ser 277:1–12

Kennedy H, Thomas DN, Kattner G, Haas C, Dieckmann GS (2002) Particulate organic matter in Antarctic summer sea ice: concentration and stable isotopic composition. Mar Ecol Prog Ser 238:1–13

Kottmeier ST, Grossi SM, Sullivan CW (1987) Sea ice microbial communities. VIII. Bacterial production in annual sea ice of McMurdo Sound, Antarctica. Mar Ecol Prog Ser 35:175–186

Krell A, Funck D, Plettner I, John U, Dieckmann G (2007) Regulation of proline metabolism under salt stress in the psychrophilic diatom *Fragilariopsis cylindrus* (Bacillariophyceae). J Phycol 43:753–762

Krembs C, Deming JW (2008) The role of exopolymers in microbial adaptation to sea ice. In: Margesin R, Schinner F, Marx JC, Gerday C (eds) Psychrophiles: from biodiversity to biotechnology. Springer, Heidelberg, p 247–264

Krembs C, Engel A (2001) Abundance and variability of microorganisms and transparent exopolymer particles across the ice-water interface of melting first-year sea ice in the Laptev Sea (Arctic). Mar Biol 138:173–185

Krembs C, Eicken H, Junge K, Deming JW (2002) High concentrations of exopolymeric substances in Arctic winter sea ice: implications for the polar ocean carbon cycle and cryoprotection of diatoms. Deep-Sea Res I 49:2163–2181

Krembs C, Eicken H, Deming JW (2011) Exopolymer alteration of physical properties of sea ice and implications for ice habitability and biogeochemistry in a warmer Arctic. Proc Natl Acad Sci USA 108:3653–3658

Laws EA, Bidigare RR, Popp BN (1997) Effect of growth rate and CO_2 concentration on carbon isotopic fractionation by the marine diatom *Phaeodactylum tricornutum*.

Limnol Oceanogr 42:1552–1560

Lebaron P, Servais P, Baudoux AC, Bourrain M, Courties C, Parthuisot N (2002) Variations of bacterial-specific activity with cell size and nucleic acid content assessed by flow cytometry. Aquat Microb Ecol 28:131–140

Leppäranta M, Manninen T (1988) The brine and gas content of sea ice with attention to low salinities and high temperatures. Internal Report 88-2, Finnish Institute Marine Research, Helsinki

Lizotte MP, Sullivan CW (1992) Photosynthetic capacity in microalgae associated with Antarctic pack ice. Polar Biol 12:497–502

Martin A, Hall JA, O'Toole R, Davy SK, Ryan KG (2008) High single-cell metabolic activity in Antarctic sea ice bacteria. Aquat Microb Ecol 52:25–31

Martin A, Hall JA, Ryan KG (2009) Low salinity and high-level UV-B radiation reduce single-cell activity in Antarctic sea ice bacteria. Appl Environ Microbiol 75: 7570–7573

Martin A, McMinn A, Davy SK, Anderson MJ, Miller HC, Hall JA, Ryan KG (2012) Preliminary evidence for the microbial loop in Antarctic sea ice using microcosm simulations. Antarct Sci 24:547–553

McMinn A, Hegseth EN (2004) Quantum yield and photosynthetic parameters of marine microalgae from the Southern Arctic Ocean, Svalbard. J Mar Biol Assoc UK 84:865–871

McMinn A, Skerratt J, Trull T, Ashworth C, Lizotte M (1999) Nutrient stress gradient in the bottom 5 cm of fast ice, McMurdo Sound, Antarctica. Polar Biol 21:220–227

McMinn A, Ashworth C, Ryan KG (2000) In situ net primary productivity of an Antarctic fast ice bottom algal community. Aquat Microb Ecol 21:177–185

McMinn A, Ryan K, Grademann R (2003) Diurnal changes in photosynthesis of Antarctic fast ice algal communities determined by pulse amplitude modulation fluorometry. Mar Biol 143:359–367

McMinn A, Pankowskii A, Ashworth C, Bhagooli R, Ralph P, Ryan K (2010) In situ net primary productivity and photosynthesis of Antarctic sea ice algae, phytoplankton and benthic algal communities. Mar Biol 157:1345–1356

Meiners K, Brinkmeyer R, Granskog MA, Lindfors A (2004) Abundance, size distribution and bacterial colonization of exopolymer particles in Antarctic sea ice (Bellingshausen Sea). Aquat Microb Ecol 35:283–296

Meiners KM, Krembs C, Gradinger R (2008) Exopolymer particles: microbial hotspots of enhanced bacterial activity in Arctic fast ice (Chukchi Sea). Aquat Microb Ecol 52:195–207

Meiners KM, Papadimitriou S, Thomas DN, Norman L, Dieckmann GS (2009) Biogeochemical conditions and ice algal photosynthetic parameters in Weddell Sea ice during early spring. Polar Biol 32:1055–1065

Mock T, Valentin K (2004) Photosynthesis and cold acclimation: molecular evidence from a polar diatom. J Phycol 40:732–741

Myklestad S (1977) Production of carbohydrates by marine plankton diatoms. II. Influence of the N/P ratio in the growth medium on the assimilation ratio, growth rate, and production of cellular and extracellular carbohydrates by Chaetoceros affinis var. willei (Gran) Hustedt and Skeletonema costatum (Grev.) Cleve. J Exp Mar Biol Ecol 29:161–179

Myklestad SM, Børsheim KY (2007) Dynamics of carbohydrates in the Norwegian Sea inferred from monthly profiles collected during 3 years at 66°N, 2°E. Mar Chem 107:475–485

Myklestad S, Holm-Hansen O, Vårum KM, Volcani BE (1989) Rate of release of extracellular amino acids and carbohydrates from the marine diatom Chaetoceros affinis. J Plankton Res 11:763–773

Oppenheim DR, Ellis-Evans JC (1989) Depth-related changes in benthic diatom assemblages of a maritime Antarctic lake. Polar Biol 9:525–532

Pakulski JD, Benner R (1994) Abundance and distribution of dissolved carbohydrates in the ocean. Limnol Oceanogr 39:930–940

Palmisano AC, Garrison DL (1993) Microorganisms in Antarctic sea ice. In: Friedmann EI (ed) Antarctic microbiology. Wiley-Liss, New York, NY, p 167–218

Palmisano AC, Sullivan CW (1983) Sea ice microbial communities (SIMCO). Polar Biol 2:171–177

Papadimitriou S, Thomas DN, Kennedy H, Kuosa H, Krell A, Dieckmann GS (2007) Biogeochemical composition of natural sea ice brines from the Weddell Sea during early austral summer. Limnol Oceanogr 52:1809–1823

Petrich C, Eicken H (2010) Growth, structure and properties of sea ice. In: Thomas DN, Dieckmann GS (eds) Sea ice, 2nd edn. Wiley–Blackwell, Oxford, p 23–77

Popp BN, Trull T, Kenig F, Wakeham SG and others (1999) Controls on the carbon isotopic composition of Southern Ocean phytoplankton. Global Biogeochem Cycles 13: 827–843

Qian J, Mopper K (1996) An automated, high performance, high temperature combustion dissolved organic carbon analyser. Anal Chem 68:3090–3097

Redfield AC, Ketchum BH, Richards FA (1963) The influence of organisms on the composition of sea-water. In: Hill MN (ed) The sea, Vol 2. John Wiley & Sons, New York, NY, p 26–77

Riebesell U, Wolf-Gladrow DA, Smetacek V (1993) Carbon dioxide limitation of marine phytoplankton growth rates. Nature 361:249–251

Riedel A, Michel C, Gosselin M (2006) Seasonal study of sea-ice exopolymeric substances on the Mackenzie shelf: implications for transport of sea-ice bacteria and algae. Aquat Microb Ecol 45:195–206

Riedel A, Michel C, Gosselin M, LeBlanc B (2007) Enrichment of nutrients, exopolymeric substances and microorganisms in newly formed sea ice on the Mackenzie shelf. Mar Ecol Prog Ser 342:55–67

Riedel A, Michel C, Gosselin M, LeBlanc B (2008) Winter-spring dynamics in sea-ice carbon cycling in the coastal Arctic Ocean. J Mar Syst 74:918–932

Ryan KG, Ralph P, McMinn A (2004) Acclimation of Antarctic bottom-ice algal communities to lowered salinities during melting. Polar Biol 27:679–686

Ryan KG, Hegseth EN, Martin A, Davy SK and others (2006) Comparison of the microalgal community within fast ice at two sites along the Ross Sea coast, Antarctica. Antarct Sci 18:583–594

Schreiber U (2004) Pulse amplitude (PAM) fluorometry and saturation pulse method. In: Papageorgiou G., Govindjee (eds) Chorophyll a fluorescence: a signature of photosynthesis. Advances in photosynthesis and respiration Series, Kluwer Academic Publishers, Dordrecht, p 279–319

Servais P, Casamayor EO, Courties C, Catala P, Parthuisot N, Lebaron P (2003) Activity and diversity of bacterial cells with high and low nucleic acid content. Aquat Microb Ecol 33:41–51

Smith REH, Demers S, Hattori H, Kudoh S and others (1995) Biological and chemical investigations of the Saroma-Resolute project in ice-covered Resolute Passage, 1992. Can Data Rep Hydrogr Ocean Sci, DFO, 137

Staats N, Stal LJ, Mur LR (2000) Exopolysaccharide production by the epipelic diatom *Cylindrotheca closterium*: effects of nutrient concentrations. J Exp Mar Biol Ecol 249:13–27

Sullivan CW, Palmisano AC (1984) Sea ice microbial communities: distribution, abundance, and diversity of ice bacteria in McMurdo Sound, Antarctica, in 1980. Appl Environ Microbiol 47:788–795

Sullivan CW, Palmisano AC, Kottmeier S, McGroath Grossi S, Moe R (1985) The influence of light on growth and development of the sea-ice microbial community of McMurdo Sound. In: Siegfried WR, Condy PR, Laws RM (eds) Antarctic nutrient cycles and food webs. Springer, Berlin, p 78–83

Taylor GT, Sullivan CW (2008) Vitamin B12 and cobalt cycling among diatoms and bacteria in Antarctic sea ice microbial communities. Limnol Oceanogr 53:1862–1877

Thomas DN, Dieckmann GS (eds) (2010) Sea ice, 2nd edn. Wiley-Blackwell, Oxford

Thomas DN, Kattner G, Engbrodt R, Giannelli V, Kennedy H, Haas C, Dieckmann GS (2001) Dissolved organic matter in Antarctic sea ice. Ann Glaciol 33:297–303

Thomson PG, Davidson AT, van den Enden R, Pearce I, Seuront L, Paterson JS, Williams GD (2010) Distribution and abundance of marine microbes in the Southern Ocean between 30 and 80°E. Deep-Sea Res II 57:815–827

Trenerry L, McMinn A, Ryan K (2002) *In situ* oxygen microelectrode measurements of bottom-ice algal production in McMurdo Sound, Antarctica. Polar Biol 25:72–80

Ugalde SC, Meiners KM, Davidson AT, Westwood KJ, McMinn A (2013) Photosynthetic carbon allocation of an Antarctic sea ice diatom (*Fragilariopsis cylindrus*). J Exp Mar Biol Ecol 446:228–235

Underwood GJC, Paterson DM (2003) The importance of extracellular carbohydrate production by marine epipelic diatoms. Adv Bot Res 40:183–240

Underwood GJC, Smith DJ (1998) Predicting epipelic diatom exopolymer concentrations in intertidal sediments from sediment chlorophyll *a*. Microb Ecol 35:116–125

Underwood GJC, Boulcott M, Raines CA, Waldron K (2004) Environmental effects on exopolymer production by marine benthic diatoms — dynamics, changes in composition and pathways of production. J Phycol 40:293–304

Underwood GJC, Fietz S, Papadimitriou S, Thomas DN, Dieckmann GS (2010) Distribution and composition of dissolved extracellular polymeric substances (EPS) in Antarctic sea ice. Mar Ecol Prog Ser 404:1–19

Underwood GJ, Aslam SN, Michel C, Niemi A and others (2013) Broad-scale predictability of carbohydrates and exopolymers in Antarctic and Arctic sea ice. Proc Natl Acad Sci USA 110:15734–15739

van der Merwe P, Lannuzel D, Mancuso Nichols CA, Meiners K and others (2009) Biogeochemical observations during the winter–spring transition in East Antarctic sea ice: evidence of iron and exopolysaccharide controls. Mar Chem 115:163–175

van Oijen T, van Leeuwe MA, Granum E, Weissing FJ, Bellerby RGJ, Gieskes WWC, de Baar HJW (2004) Light rather than iron controls photosynthate production and allocation in Southern Ocean phytoplankton populations during austral autumn. J Plankton Res 26:885–900

Vancoppenolle M, Goosse H, de Montety A, Fichefet T, Tremblay B, Tison JL (2010) Modelling brine and nutrient dynamics in Antarctic sea ice: the case of dissolved silica. J Geophys Res 115:C02005, doi:10.1029/2009JC005369

Vancoppenolle M, Meiners KM, Michel C, Bopp L and others (2013) Role of sea ice in global biogeochemical cycles: emerging views and challenges. Quat Sci Rev 79:207–230

Waite AM, Olson RJ, Dam HG, Passow U (1995) Sugar-containing compounds on the cell surfaces of marine diatoms measured using concanacalin A and flow cytometry. J Phycol 31:925–933

Wedborg M, Hoppema M, Skoog A (1998) On the relation between organic and inorganic carbon in the Weddell Sea. J Mar Syst 17:59–76

Wolfstein K, Stal LJ (2002) Production of extracellular polymeric substances (EPS) by benthic diatoms: effect of irradiance and temperature. Mar Ecol Prog Ser 236:13–22